Optics & Laser Technology 42 (2010) 274–279

Contents lists available at ScienceDirect

Optics & Laser Technology

journal homepage: www.elsevier.com/locate/optlastec

# Coherent combining of a seven-element hexagonal fiber array

Xinyan Fan [a,*], Jingjiao Liu [a,b], Jinsheng Liu [a], Jingli Wu [c]

[a] National key Laboratory of Tunable Laser Technology, Harbin Institute of Technology, Harbin 150001, China
[b] North China Institute of Electronic Equipment, Beijing 100083, China
[c] Changchun Institute of Optics, Fine Mechanics and Physics, Chinese Academy of Sciences, Changchun 130033, China

ARTICLE INFO

*Article history:*
Received 12 November 2008
Received in revised form
10 April 2009
Accepted 1 July 2009
Available online 5 August 2009

*Keywords:*
Coherent combining
Fiber array
Fill factor

ABSTRACT

The coherent combination of the outputs from a seven-element hexagonal fiber array with a hexagonal prism is described. The fill factor of the coherent array achieves 0.6. A total of 0.40 of the energy is contained in the central lobe and the Strehl ratio is 0.91. A theoretical model of the hexagonal fiber array is established based on Fraunhofer diffraction theory. The far field distribution of the hexagonal fiber array is presented. The effects of fill factor and phase errors on far field distribution are analyzed and simulated.



## 1. Introduction

The coherent combination of multiple fiber laser sources is becoming a viable option to realize high-power and high-brightness laser output. Compared with wavelength beam combining, in a coherent combination system both power and brightness are scaled. In recent years, various coherent combining techniques have been brought forward and investigated to obtain near-ideal coherently combined beams. There are excellent reviews on the progress of coherent combining [1]. Generally speaking, coherent combining implementations on fiber laser arrays can be divided into two subsets, characterized by the phase-locking technique used: active phasing and passive phasing. The active phasing implementations mostly employ master oscillator power amplifier (MOPA) architectures [2], which require additional phase-locking electronics. The passive phasing implementations are generally explained by the self-organized mechanism, including interferometric resonators [3], the self-Fourier resonator [4], or fiber couplers [5]. Most of the above-mentioned investigations have been experimentally demonstrated.

Many theoretical and experimental demonstrations of the active phasing coherent combining system with MOPA architecture have been reported. The prior research was mainly focused on a 1-D linear or 2-D square distribution array. The far field intensity distribution was mostly described by the propagation theory of the Gaussian beam [6] or Huygens–Fresnel integral [7]. For the MOPA architecture, phase controlling electronics and unit fill factor are two major challenges. The conventional v-groove array [2] is generally employed to obtain high fill factor, but requires high processing and alignment precision. Three main phase controlling techniques are adaptive phase-locking [8], heterodyne phase-locking [2] and self-referenced phase-locking [9] techniques. The hill climbing technique [10], as a classical adaptive technique, is a popular technique for easy implementation and element number scaling.

In this paper, a seven-element hexagonal fiber array that employs a hexagonal prism as the combining component and that uses the hill climbing method as the phase controlling technique is described. The architecture greatly improves the fill factor and the energy contained in the central lobe. Secondly, a theoretical model of the far field intensity distribution of a hexagonal fiber array is presented using Fraunhofer diffraction theory. The effects of fill factor and phase errors on far field intensity distribution are numerically analyzed and simulated. The experimental far field intensity distribution is well matched with the simulation results. At the end, we give a brief conclusion of the experimental results and the scaling ability of the architecture.

## 2. Experiment

In order to improve the fill factor of present MOPA architectures, we develop a seven-element hexagonal fiber coherent array employing a hexagonal prism. Fig. 1 shows a schematic of the experimental setup. The master oscillator (MO) is a single frequency non-planar ring oscillator (NPRO) with diode pumped Nd:$YVO_4$, which is operated at 1064 nm with output power in the range 0–1000 mW. The line width is less than 5 KHz. The MO is

* Corresponding author. Fax: +86 10 64390568.
*E-mail address:* fanshong_02@yahoo.com.cn (X. Fan).

0030-3992/$ - see front matter © 2009 Elsevier Ltd. All rights reserved.
doi:10.1016/j.optlastec.2009.07.004

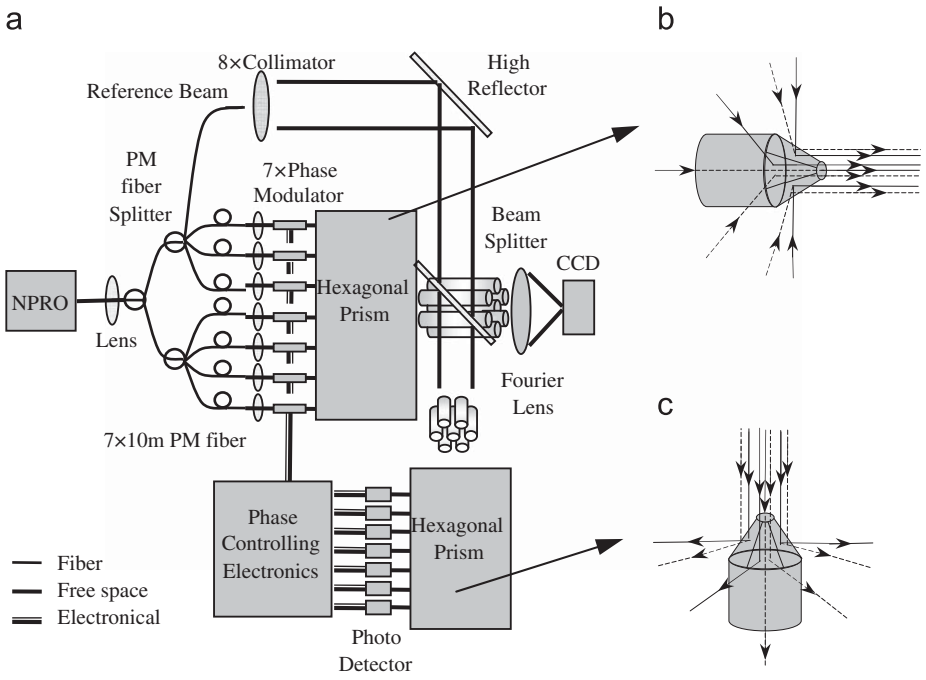


**Fig. 1.** Schematic of the seven-element hexagonal fiber coherent array: (a).experimental setup, (b). combining component and (c). splitting component.

coupled into a $1\times8$ PM fiber splitter and split into one reference arm and seven signal arms. The $1\times8$ PM fiber splitter is composed of one $1\times2$ splitter and two $1\times4$ splitters. The signal arms are seven 10 m lengths of panda polarization maintaining (PM) fiber of 6.6 μm core diameter. The power of each signal arm is 100 mW which is adjusted by different attenuators. After collimating, the seven signal arms each pass through a lithium niobate phase modulator. A hexagonal prism is employed as a combining component to transform the seven signal arms into a seven-element array with a fill factor of 0.6. Similarly, another hexagonal prism splits the seven-element array into seven beams each of which is monitored on by a photodiode. A sample of each signal arm is interfered with the reference arm to measure the phase of that arm relative to the reference arm. The phase controlling electronics are comprised of seven parallel electronics which, respectively, detect and adjust the phase of each signal arm, then feedback a control voltage to the corresponding phase modulator in an arm. The far field pattern is imaged in the focal plane of a Fourier lens.

Regarding the hexagonal distribution array and the precise position requirement, we design a hexagonal prism as shown in the illustration of Fig. 1. The hexagonal prism is cut with six 45° inclined planes with 99.9% golden reflective coating and one central through hole. The principle of the hexagonal prism as combining component is as following: six beams incident into the prism with 45° incidence angle in the plane perpendicular to the paper, then reflect to horizontal direction. The central beam exits through the central hole. Then the seven-element beams are transformed to an array of seven parallel beams with a certain fill factor. In the same way, vertically incident to the hexagonal prism, the seven parallel beams array will split into seven different directions. The collimated beam diameter is 2.4 mm, and the spacing between the beams is 4 mm.

As a note, the fill factor of the seven-element hexagonal fiber array can be as high as 0.6, which is an advantage of our coherent combining system. Compared with traditional v-groove array [2] with its precise accuracy requirement, the hexagonal prism has the advantage of inherent high alignment accuracy as a combining architecture, and acquires a perfect detecting precision as a splitting architecture. Moreover, the array could scale to large element number by adding another hexagonal prism with larger central through hole, or by cutting the prism such that it has a larger number of reflecting surfaces.

We employ a relatively easy phase controlling technique which is called the hill climbing method [10]. The hill climbing phase detection is a technique that automatically optimizes the control point by software control. Firstly, a triangular wave is applied to the phase modulator periodically. After sweeping several periods, a maximal output value is created representing the maximal intensity of the interference fringe. A reference voltage is set by a certain percentage of the maximal voltage by the software. The detected real-time voltage is compared with the reference voltage resulting in a control voltage. The control voltage is fed back to the phase modulator for each signal arm to correct the phase of that arm. The feedback process cycles until the interference intensity becomes stable. The seven phase controlling electronics are implemented in parallel. In this way, all of the output phases of the signal arm are exactly locked with the reference arm. In our seven-element hexagonal fiber array system, the phase control electronics is designed to operate at 10 KHz and the control precision could reach $\lambda/12$.

It should be noted that we arrange the elements in hexagonal distribution. As a typical two-dimensional array, the hexagonal array has a good symmetry approximate to a circle, and can contain more elements in a given area than other array shapes. The far field intensity distribution of the hexagonal fiber array will be analyzed in Section 4.

## 3. Experiment results

The key metrics for the far field distribution of the coherent combining system are the energy contained in the central lobe [11] and Strehl ratio [1]. The energy contained in the central lobe is defined as the energy in the central lobe to the whole energy. Strehl ratio is defined as the ratio of the on-axis intensity to that of an ideal equal-power top-hat beam. It is particularly useful for describing the phase errors of the phase control electronics. In this

paper, we employ these two metrics to express the far field distribution properties of coherent combining system, which are also the most authorized evaluating parameters in coherent combining system.

The experimental result of the seven-element hexagonal fiber array is shown in Fig. 2. The power of combining beam is measured as 620 mW and the combining efficiency is 88.57%. The power in the central lobe is 240 mW. Calculated from the grayscale of the CCD photos, with a fill factor of 0.6, the energy contained in the central lobe is 0.40 and the Strehl ratio is 0.91.

## 4. Hexagonal fiber array

The profile of a hexagonal fiber array is shown in Fig. 3. The array consists of $N$ elements. We suppose that $m$ is the surrounding ring number, for one element array $m=0$, and $n$ is the element number in the $m$th surrounding ring. The separation distance among the adjacent elements is $d$. Then the position coordinate $(x_{mn}, y_{mn})$ of the $n$th element in the $m$th surrounding ring can be expressed as

$$x_{mn} = md\cdot\ \cos\left[(n-1)\frac{2\pi}{6m}\right],$$

$$y_{mn} = md\cdot\ \sin\left[(n-1)\frac{2\pi}{6m}\right], \tag{1}$$

while the element number $N$ could be expressed as

$$N = 1+\sum_{m=0}^{M} 6m. \tag{2}$$

To calculate the intensity distribution in the far field, we assumed that each element is identical with a Gaussian amplitude distribution with the waist radius of $\omega_0$, and the wave fronts are collimated and co-aligned in the output plane. Then the field distribution in the output plane is give by

$$U(x,y) = \sum_{m=0}^{M}\sum_{n=1}^{6m} A_{mn}\exp\left[-\frac{(x-x_{mn})^2+(y-y_{mn})^2}{\omega_0^2}+i\phi_{mn}\right]$$

$$= \sum_{m=0}^{M}\sum_{n=1}^{6m} A_{mn}\exp\left(-\frac{x^2+y^2}{\omega_0^2}+i\phi_{mn}\right)^{*}\delta(x-x_{mn},y-y_{mn}), \tag{3}$$

where $A_{mn}$ is the axial amplitudes, $\phi_{mn}$ the initial phase, and $^*$ the convolution operator.

Based on Fraunhofer diffraction theory, the far field distribution could be expressed by the Fourier transform of the electric field distribution at the output plane:

$$U(f_{x'},f_{y'}) = \frac{\exp(jkz')}{j\lambda z'}\exp\left[jk\left(\frac{x'^2+y'^2}{2z'}\right)\right]$$

$$\times\int_{-\infty}^{+\infty}\int_{-\infty}^{+\infty}\sum_{m=0}^{M}\sum_{n=1}^{6m} A_{mn}\exp\left(-\frac{x^2+y^2}{\omega_0^2}+i\phi_{mn}\right)^{*}\delta(x-x_{mn},y-y_{mn})$$

$$\times\exp[-i2\pi(f_{x'}x+f_{y'}y)]dx\,dy, \tag{4}$$

where $(x, y)$ is the coordinate system at the output plane, $(x', y')$ is the coordinate system of far field, $f_{x'}\approx\theta_x/\lambda$ and $f_{y'}\approx\theta_y/\lambda$ are spatial

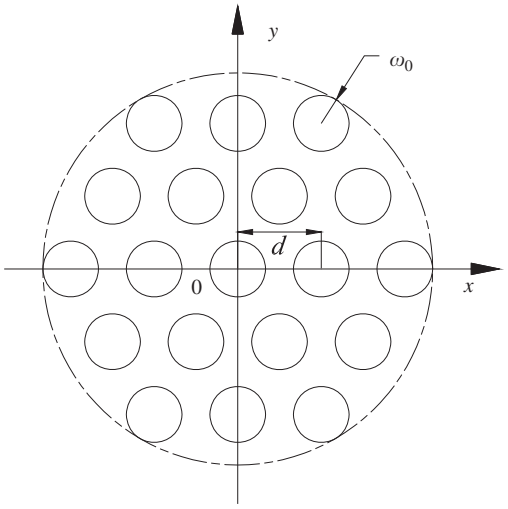


**Fig. 3.** Schematic diagram of the hexagonal fiber array. The element is with waist radius of $\omega_0$. The separation distance among the adjacent elements is $d$.

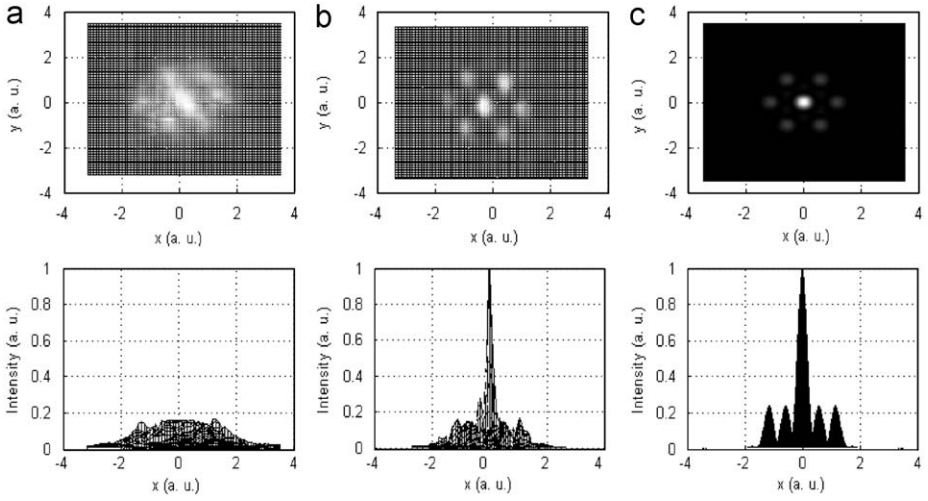


**Fig. 2.** The far field distribution of the seven-element hexagonal fiber array: (a). experimental measured incoherent combination, (b). experimental measured coherent combination and (c). theoretical simulation coherent combination. The upper is the CCD photo, and the lower is the far field intensity profile along the $x$-axis. The far field peak intensity of measured coherent combination is 6.4 times of incoherent combination. The experimental energy contained in the central lobe is 0.40, while the theoretical value is 0.51, and the Strehl Ratio is 0.91.

frequencies. Then, omitting the constant term, the far field intensity is given by

$$I(\theta_x,\theta_y)\propto\left|\sum_{m=0}^{M}\sum_{n=1}^{6m}A_{mn}\exp\{i[k(x_{mn}\theta_x+y_{mn}\theta_y)-\phi_{mn}]\}\right|^2 \times\exp\left[-\frac{k^2\omega_0^2}{2}(\theta_x^2+\theta_y^2)\right]. \quad (5)$$

This equation shows that the far field intensity is represented by the product of the near field distribution function and the single element far field distribution with Gaussian function. It can be seen that Eq. (5) contains the information of amplitude, phase and position of single element, and contains the array distribution structure and separation distance in near field. Eq (5) is appropriate to analyze the effect of these parameters on the far field intensity distribution.

### 4.1. Fill factor

The far field intensity distribution is degraded by errors in the relative phase control, amplitude control, polarization control, element beam pointing and a less-than-unity fill factor. One difficulty for acquiring ideal coherent combining is the control of the phase. Another source of non-ideal performance is a less-than-unity fill factor, so the primary focus here is on these two factors.

We take the seven-element array as an example to simulate the numerical calculation of the far field distribution. The parameters used in simulation are $m=1$, $N=7$, $\lambda=1.064\,\mu m$, $\omega_0=1.2\,mm$, $A_{mn}=1$. $d$ and $\phi_{mn}$ are varied.

Consider the effect of a less-than-unity fill factor on the far field intensity. Here, the fill factor is calculated by dividing the spot size of the element aperture by the distance of the elements, that is $f=2\omega_0/d$. The far field intensity of the seven-element hexagonal array is

$$I(\theta_x,\theta_y)\propto\left|1+2\cos(kd\theta_x)+4\cos\left\{kd\left[\cos\left(\frac{\pi}{3}\right)\theta_x+\sin\left(\frac{\pi}{3}\right)\theta_y\right]\right\}\right|^2 \times\exp\left[-\frac{k^2\omega_0^2}{2}(\theta_x^2+\theta_y^2)\right]. \quad (6)$$

Fig. 4 shows the far field intensity profile of the seven-element hexagonal fiber array with different fill factors. We vary the fill factor by increasing the element separation distance, which can also be realized by reducing the spot size of element aperture. It can be seen that the fill factor affects the far field intensity patterns in terms of the central lobe angular width and number of side lobes. As the fill factor reduces, the energy contained in the central lobe reduces, which causes the far field brightness to weaken. The effect of fill factor on the energy contained in the central lobe is given in Fig. 5. The energy contained in the central lobe reduces almost linearly with the fill factor reduction. For a fill factor of 0.6, the ideal energy contained in the central lobe is 0.51.

As a note, the effect of the fill factor on the far field intensity distribution analyzed by Fraunhofer diffraction intensity is different from the Gaussian beam propagation theory in Ref. [9]. The latter assumed a Gaussian beam with some divergence angle, and calculated the intensity distribution of the overlapping beams at a long distance from the near field (20 m in Ref. [9]), which is not the true far field intensity distribution, while Eq. (5), deduced from Fraunhofer diffraction theory, is expressed by a Fourier transform of the near field distribution, which is the true far field in infinite distance. The two simulation results from these two

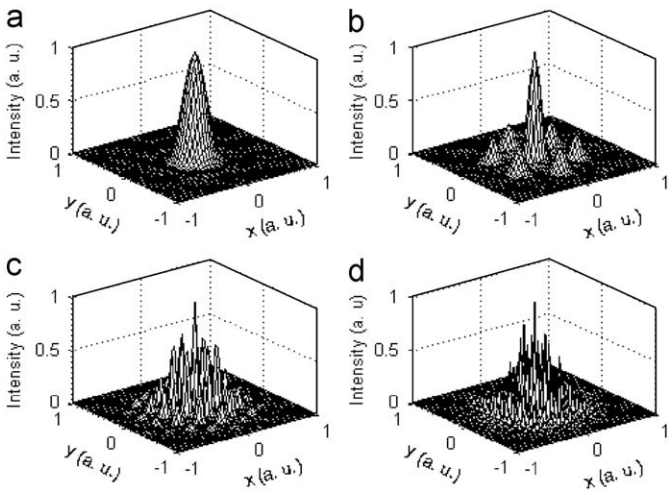


**Fig. 4.** The far-field profile of different fill factors. The simulation parameters are $m=1$, $N=7$, $\omega_0=1.2\,mm$, $\lambda=1.064\,\mu m$, $A_{mn}=1$ and $\varphi_{mn}=1$. (a) $d=2.4\,mm$, $f=1.0$; (b) $d=4.8\,mm$, $f=0.5$; (c) $d=9.6\,mm$, $f=0.25$ and (d) $d=24\,mm$, $f=0.1$.

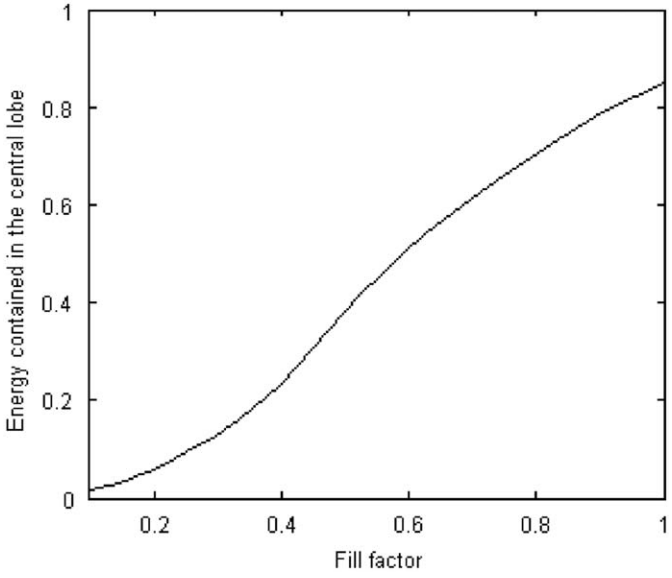


**Fig. 5.** The effect of fill factor on the energy contained in the central lobe for a seven-element hexagonal fiber array.

theories differ slightly. In Fig. 4 of Ref. [9], the reduction of fill factor just enlarges the peak of side lobes, and makes no change to the number of side lobes. A smaller fill factor should increase the number of side lobes and reduce the energy contained in the central lobe, as shown in Fig. 4. Therefore, we consider the Fraunhofer diffraction theory is a more appropriate approach for simulation of the far field intensity distribution of a coherent combining system.

### 4.2. Phase errors

In a fiber laser coherent combining system, the environmental vibration, the changes in temperature or the pumping current may all introduce phase noise. Furthermore, as the output power is increased, the phase noise worsens. Therefore, the element phase $\phi_{mn}$ is a random variable of statistical independence [12]

and is assumed as zero-mean Gaussian variable

$$f(\phi_{mn}) = \frac{1}{\sqrt{2\pi}\sigma_\phi}\exp\left(-\frac{\phi_{mn}^2}{2\sigma_\phi^2}\right), \tag{7}$$

where $\sigma_\phi$ is the relative root-mean-square (rms) of $\phi_{mn}$. Then the far field intensity is

$$I(\theta_x,\theta_y) \propto \left\{7(1-\exp(-\sigma_\phi^2)) + \exp(-\sigma_\phi^2)\left|1+2\cos(kd\theta_x)+4\cos\left\{kd\left[\cos\left(\frac{\pi}{3}\right)\theta_x+\sin\left(\frac{\pi}{3}\right)\theta_y\right]\right\}\right|^2\right\} \times\exp\left[-k^2\omega_0^2(\theta_x^2+\theta_y^2)\right]. \tag{8}$$

Eq. (8) shows that the far field intensity is degraded by two components, the intensity is reduced by a factor of $\exp(-\sigma_\phi{}^2)$ and there is a constant pedestal of $7(1-\exp(-\sigma_\phi{}^2))$. When $\sigma_\phi = 0$, the intensity scales perfectly by a factor $N^2 = 49$. When $\sigma_\phi \to \infty$, the intensity adds incoherently and the intensity just scales in proportion to the number of elements. Fig. 6 shows the far field intensity profile with different phase errors of $\sigma_\phi = 0, 2\pi/10, 2\pi/5, 2\pi$. It shows that the phase errors have no effect on the distribution of the central and side lobes, rather they disperse a fraction of the energy from the central lobe into the side lobes.

In a coherent combining system with rms phase error of$\sigma_\phi$, the Strehl ratio of the far field intensity is given by

$$S = \exp(-\sigma_\phi^2) + \frac{1}{7}[1-\exp(-\sigma_\phi^2)] \tag{9}$$

The effect of phase errors on the Strehl ratio for three different element arrays, $N = 7$, $N = 37$ and $N = 91$ is shown in Fig. 7. It can be seen that the increase of the rms phase error $\sigma_\phi$ and element number will cause the Strehl ratio to be degraded. For the seven-element hexagonal fiber coherent array, to limit the degradation of the Strehl ratio caused by phase errors to 0.8, the rms phase errors must be limited to $\sim\lambda/12$ or better. The requirement of phase errors is slightly different from Refs. [1,9,11].

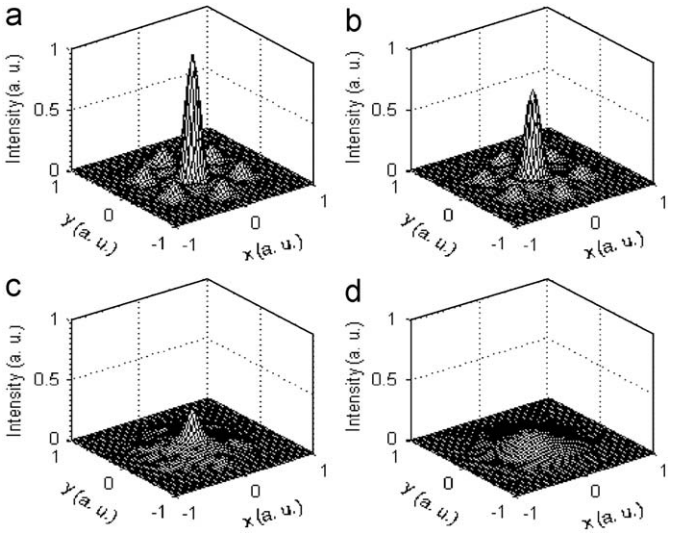


**Fig. 6.** The far-field profile of different variance of phase errors. The parameters are $m = 1$, $N = 7$, $\omega_0 = 1.2$ mm, $\lambda = 1.064\,\mu$m, $A_{mn} = 1$, $d = 4.8$ mm and $f = 0.5$. (a) $\sigma_\varphi = 0$; (b) $\sigma_\varphi = 2\pi/10$; (c) $\sigma_\phi = 2\pi/5$ and (d) $\sigma_\varphi = 2\pi$.

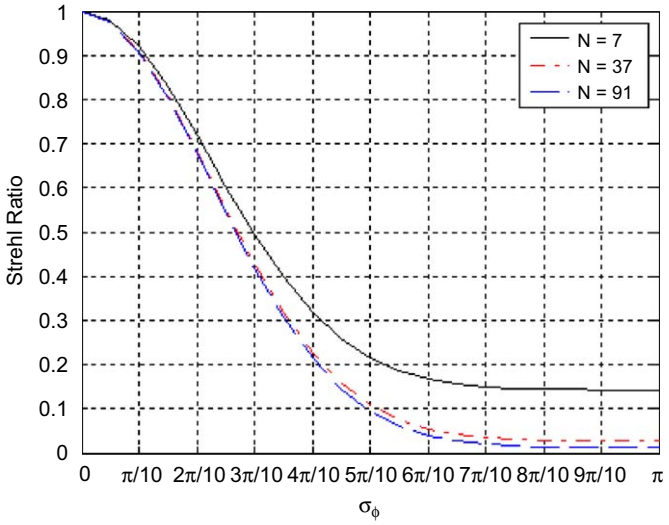


**Fig. 7.** The effect of phase errors on Strehl ratio for three different element number arrays. The solid line (black) is $N = 7$, the dashed line (red) is $N = 37$ and the dash-dot line (blue) is $N = 91$. (For interpretation of the references to colour in this figure legend, the reader is referred to the web version of this article).

### 4.3. Discussion

As shown in Fig. 2, the experimental results agree with the theoretical analysis using Fraunhofer diffraction theory. There is some difference due to the alignment errors and phase controlling accuracy, for example, the measured coherent far field distribution has no zero points. The far field peak intensity of the measured coherent combination is 6.4 times of incoherent combination. The energy contained in the central lobe is 0.40, while the ideal energy contained in the central lobe is 0.51.

## 5. Conclusions

In this paper, we present a seven-element hexagonal fiber coherent array employing a hexagonal prism. The hexagonal prism is used as the combining and the splitting component to obtain high fill factor. The phase controlling electronics employed the hill climbing method. We obtained a seven-element hexagonal fiber array with fill factor as high as 0.6 and in the far field distribution the energy contained in the central lobe is 0.40 and the Strehl ratio is 0.91. The hexagonal fiber array has an advantage of high fill factor. The basic aim of coherent combination is to centralize as much energy as possible in the central lobe and the requirement of the fill factor in MOPA architecture is extremely significant. In our coherent combining architecture with a high fill factor, the power and element number may be scaled by superposing two or more hexagonal prisms of different sizes.

The far field intensity of the hexagonal fiber array is studied by Fraunhofer diffraction theory. The effects of the fill factor and phase errors on far field intensity pattern are theoretically analyzed and simulated. The simulation results show that the non-unity fill factor reduces the energy contained in the central lobe and increases side lobe numbers. The phase errors attenuate the on-axis intensity and disperse the energy in the central lobe into the side lobes.

As a note, we employed a 10 m length of PM fiber to substitute the fiber amplifier to demonstrate the advantage of the hexagonal prism to improve fill factor and energy contained in the central lobe. Theoretically, these two systems with same combining

components should have identical far field intensity distributions. However, the phase noise of PM fiber amplifying the laser signal would be expected to be worse than the 10 m of fiber with no pumping or amplification.

## Acknowledgement

This work is sponsored by the Major Project of Chinese National Programs for Fundamental Research and Development (no. 61359030201).

## References

[1] Fan TY. Laser beam combining for high-power high radiance sources. IEEE J Quantum Electron 2005;11:567–77.
[2] Anderegg J, Brosnan S, Weber M, Komine H, Wickham M. 8-watt coherently phased 4-element fiber array. Proc SPIE 2003;4974:1–6.
[3] Sabourdy D, Kermene V, Desfarges-Berthelemot A, Lefort L, Barthelemy A. Efficient coherent combining of widely tunable fiber lasers. Opt Express 2003;11:87–97.
[4] Corcoran CJ, Durville F. Experimental demonstration of a phase-locked array using a self-Fourier cavity. Appl Phys Lett 2005;86:201118-1–3.
[5] Bruesselbach H, Jones DC, Mangir MS, Minden M, Rogers JL. Self-organized coherence in fiber laser arrays. Opt Lett 2005;30:1339–41.
[6] Li YZ, Qian LJ, Lu DQ, Fan DY, Wen SC. Coherent and incoherent combining of fiber array with hexagonal ring distribution. Opt Laser Technol 2007;39:957–63.
[7] Jones DC, Scott AM, Clark S, Stace C, Clarke RG. Beam steering of a fiber bundle laser output using phased arrays techniques. Proc SPIE 2004;5335:125–31.
[8] Bruesselbach H, Minden ML, Wang SQ, Jones DC, Mangir MS. A coherent fiber array based laser link for atmospheric aberration mitigation and power scaling. Proc SPIE 2004;5338:90–101.
[9] Shay TM. Theory of electronically phased coherent beam combination without a reference beam. Opt Express 2006;14:12188–95.
[10] Xiao R, Hou J, Jiang ZF, Lu QS. Coherent combining and closed loop controlling of two fiber lasers. High Power Laser Part Beams 2007;19:31–3.
[11] Zhou P, Liu ZJ, Xu XJ, Chen ZL. Numerical analysis of the effect of aberrations on coherently combined fiber laser beams. Appl Opt 2008;47:3350–9.
[12] Nabors CD. Effects of phase errors on coherent emitter arrays. Appl Opt 1994;33:2284–9.